# PAH radiative cooling and fragmentation kinematics studied within an electrostatic ring

R. Brédy, C. Ortega, J. Ji, C. Chen, J. Bernard, Abdul-Rahman Allouche, C. Joblin, A. Cassimi, S. Martin

# PAH radiative cooling and fragmentation kinematics studied within an electrostatic ring



Journal of Physics: Conference Series **583** (2015) 012042 doi:10.1088/1742-6596/583/1/012042

# PAH radiative cooling and fragmentation kinematics studied within an electrostatic ring

**R Brédy[1], C Ortéga[1], M Ji[1], L Chen[1], J Bernard[1], A R Allouche[1], C Joblin[2], A Cassimi[3] and S Martin[1]**

[1]Institut Lumière Matière, UMR5306 Université Lyon 1-CNRS, Université de Lyon 69622 Villeurbanne cedex, France
[2]Université de Toulouse, UPS-OMP, IRAP, Toulouse, France
[3]CIMAP, GANIL Université de CAEN, Bd. H. Becquerel, Caen, France

E-mail: richard.bredy@univ-lyon1.fr

**Abstract**. Radiative cooling of polycyclic aromatic hydrocarbon (PAH) cations has been studied using a compact electrostatic ion storage ring, the Mini-Ring, in a time range up to 8 ms. The time evolution of the internal energy distribution of the ensemble of stored ions shows evidences of fast cooling which is attributed to the fluorescence from thermally excited electronic states. The internal energy distribution was probed by inducing unimolecular dissociation with single-photon absorption at given storage times. Information on the fragmentation kinematics and the dissociation channels were obtained by analyzing the image of the emitted neutrals detected with a time and position sensitive detector.

## 1. Introduction

Interests for polycyclic aromatic hydrocarbons (PAH) have been developed since almost thirty years as these molecules are considered as good candidates to explain the unidentified infrared emission bands observed in some interstellar regions [1]. However, this commonly accepted PAH hypothesis could not yet be confirmed unambiguously and complex related PAH species including grains [2], fullerenes [3] and organic nanoparticles [4, 5] are considered as well. Numerous experimental and theoretical studies have been conducted to explain formation and survival of PAH in the interstellar medium [6, 7]. For vibrationally excited molecules competition between the internal energy relaxation mechanisms such as fragmentation and radiative cooling is a key parameter to understand their survival in a highly isolated environment as in space. It is now well known that the main dissociation channels of PAH are the loss of hydrogen (H, $H_2$) and acetylene ($C_2H_2$) depending on the size and internal energy of the molecule [8-10]. Regarding the radiative cooling mechanisms of small molecules, infrared (IR) emission due to vibrational transitions in the electronic ground state is usually considered as a slow process. For PAH the average IR radiative cooling rate has been calculated to be of the order of 2 $s^{-1}$ nearly independent on the size and internal energy of the PAH [11]. However, evidences of fast radiative cooling have been observed very recently for anion clusters [12, 13] and anthracene cations [14] using ion storage techniques. This fast cooling was attributed to fluorescence emission from low lying electronic excited states predicted by Leger et al. [7, 11]. This process is

induced by inverse internal conversion (IIC) which converts vibrational excitation energy stored in the electronic ground state to electronically excited states. Due to the high spontaneous electronic transition rates, in the order of $10^6$-$10^7$ $s^{-1}$ for anthracene cation, fast electronic transition can occur and the energy release by the emitted fluorescence photon ($h\nu_{elec}$=1.7eV for anthracene) is much larger than for the emission of a single IR photon (typically 0.1-0.2 eV). A first indirect evidence of the contribution of the electronic transition to the cooling has been provided for anthracene cation by Boissel et al. [11]. They needed to include the electronic transition process in their numerical simulations in order to reproduce the measured photofragmentation efficiency curve of the cold trapped ions after irradiation with a continuous and filtered visible light emitted from a Xenon arc lamp. The fast cooling rate of anthracene cation could be measured only recently by following the time evolution of the internal energy distribution (IED) of an ensemble of ions stored inside a storage ring [14, 15].

In this paper we report on the measurement of the population decay of anthracene cations at a given internal energy by analyzing the shift of the IED as a function of time. This population decay is directly related to the radiative cooling mechanism and could be compared with the calculated fluorescence emission rate due to the electronic transition. The IED of the ensemble of the stored ions was probed using laser induced dissociation and preliminary results on the fragmentation kinematics of other PAH cations (naphthalene, pyrene) are also presented.

## 2. Radiative cooling of anthracene cations

The radiative cooling of PAH was studied using an electrostatic ion storage ring, the Mini-Ring [14-17]. Anthracene molecules ($C_{14}H_{10}$) were ionized in an Electron Cyclotron Resonance (ECR) ion source creating an ensemble of ions with a broad IED. After extraction and acceleration of the ion beam to 12keV kinetic energy, a bunch of anthracene cations (1µs width) was injected inside the ring and stored up to 8ms with a 6.5 µs revolution period. The pressure inside the Mini-Ring vacuum chamber was maintained under 2 $10^{-9}$ mbars to limit probability of collision with the residual gas hence ensuring a storage lifetime up to 300 ms. The evolution of the IED of the stored ions is complex and includes the depletion of the high energy population due to the delayed dissociation as well as the shift of the population toward lower energy governed by the radiative cooling mechanisms. Neutral fragments emitted due to unimolecular dissociation were detected as a function of the storage time by a time and position sensitive detector (PSD) facing one of the straight line of the stored ion trajectory. After dissociation, the daughter ions were quickly ejected out of the ring due to the decrease of their kinetic energy which did not fulfil the stable storage conditions anymore. For anthracene cations previous results indicates that the dissociation process is quenched by the radiative cooling for time t>3ms [14, 15]. Therefore, if collisions with the residual gas is neglected, for time t>3ms further evolution of the high energy part of the IED can be attributed to the radiative cooling. In this time range, the IED was probed at a controlled storage time $t_{laser}$ by merging a nanosecond laser UV pulse ($h\nu$=3.5eV, 3$^{rd}$ harmonic of a 1kHz Nd-YAG OPO Laser) with the stored ion bunch in order to induce dissociation. To ensure single photon absorption condition, the pulse energy was controlled to be about 300 µJ/pulse. As discussed in [15] the laser wavelength has to be chosen carefully in order to bring the high-energy edge of the IED inside the sensitive energy window of the experiment. Indeed, the decay of the enhanced neutral yield induced by the photon absorption and detected with the Mini-Ring setup was sensitive only to dissociation processes of anthracene cations with energy between 9 and 10.5 eV. The IED after laser excitation was determined by analyzing the decay profile. A simulated decay curve was calculated based on the statistical dissociation rate as a function of the internal energy of anthracene [18] and a modeled IED g*(E,t) after laser excitation. The experimental neutral decay curve was fitted by varying the parameters of the modeled g*(E,t). Assuming the energy dependence of the absorption efficiency to be rather weak in the considered energy range, the IED before laser excitation g(E,t) was then obtained by subtracting the energy $h\nu$=3.5eV of the absorbed photon $g(E,t) = g^*(E,t) - h\nu$.

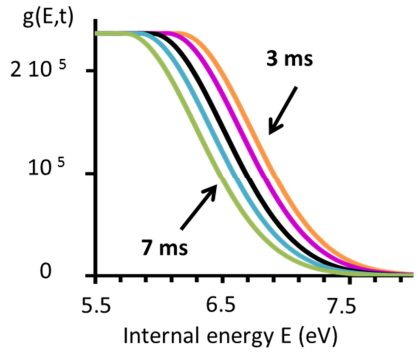


**Figure 1**. Internal energy distribution g(E,t) of the stored ions at 3, 4, 5, 6 and 7 ms of storage time.

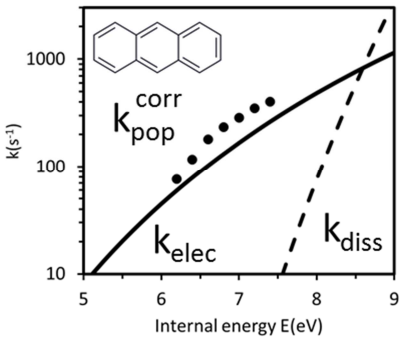


**Figure 2**. Symbols: population decay rates corrected from the IR contribution, full line: theoretical electronic transition rate for fluorescence emission, dash line: dissociation rate

In this work, the IED was modelled using a half Gaussian function for the high energy part and a constant function for the low energy part. The shape of this modelled IED is not unique and different functions were tested. However the fit of the experimental data is very sensitive to the shape of the high-energy edge of the IED and the half Gaussian shape led to the best fit. The evolution of the IED before photon absorption g(E,t) is presented in figure 1 for storage time between 3 and 7 ms. As expected, g(E,t) shifted toward lower energy with increasing storage time. In the considered time range a shift $\Delta E$=-0.5eV was measured at an average internal energy <E>=6.8 eV leading to a mean cooling rate $k_{cool}=<E>^{-1} |\Delta E/\Delta t| = 18s^{-1}$. This cooling rate is much higher than the expected cooling rate for IR emission $k_{cool,IR} = 2s^{-1}$ calculated by Boissel et al. [11]. At 7eV, the cooling $[\Delta E/\Delta t]_{IR}$ = 14eV/s due to IR emission represents roughly 10% of the total measured value $[\Delta E/\Delta t]_{mes}$ = 125eV/s. Therefore the observed fast cooling cannot be attributed only to emission from vibrational transitions which appeared to be a minor process at the considered energies. The shift toward lower energy of the IED induced ion population decay at a given internal energy E. The population decays measured at E=6.2 up to 7.2 eV follow an exponential decay law and the population decay rates $k_{pop}$ range from $85s^{-1}$ up to $390s^{-1}$, respectively. The contribution $k_{pop,IR}$ of the IR emission to this population decay rate depends on the energy but also on the shape of the IED. It was found that $k_{pop,IR}$ is proportional to $k_{pop}$ with a coefficient corresponding to the ratio $[\Delta E/\Delta t]_{IR}/[\Delta E/\Delta t]_{mes}$ = 0.1. The population decay rates corrected from the IR contribution $k_{pop}^{corr} = k_{pop} - k_{pop,IR}$ are plotted in figure 2. Considering radiative cooling due to the electronic transitions, the emission of a fluorescence photon of energy $h\nu_{elec}$ induces population decay at the energy E and an increase of the population at the energy E- $h\nu_{elec}$. As a first approach, the increase of the population at the energy E due to fluorescence from molecular ions at energy E+$h\nu_{elec}$ is considered negligible due to the high dissociation probability in the considered energy range (7+1.7=8.7eV). Considering only the first electronic excited state, the theoretical rate $k_{elec}$ of emission of a fluorescence photon $h\nu_{elec}$=1.7eV was calculated by the product of the probability of presence in the excited state by the Einstein coefficient of the transition [11]. Results are potted in figure 2 together with the dissociation rate for comparison. From figure 2 it can be noticed that the fast measured population decay rate $k_{pop}^{corr}$ is much higher than the dissociation rate $k_{diss}$ and is in fairly good agreement with the theoretical electronic transition rate $k_{elec}$. Therefore the observed fast cooling is attributed to the predicted fluorescence emission from thermally excited electronic states. It is noteworthy that this cooling process is expected to depend strongly on the electronic structure of the molecular ion. Results obtained on naphthalene cation corroborated this interpretation. The importance

of low lying electronic states in the radiative cooling process was also confirmed very recently by the observation of a drastic change in the cooling of small anion clusters $C_6^-$ and $C_6H^-$ [13].

## 3. Fragmentation kinematics

Determination of the IED through the decay of the neutral signal as a function of time after the laser excitation relies on a simple unimolecular statistical dissociation model. For PAHs, the main fragmentation scheme presents a strong competition between the loss of H and $C_2H_2$. The knowledge of the branching ratios of the competitive channels as well as the evolution of the dissociation rates with the internal energy is therefore crucial to perform the analysis. In the following, preliminary results on the fragmentation kinematics of PAH are presented using the image of the neutrals impacting the PSD. Figure 3(a) presents the PSD image for neutrals emitted by stored pyrene cations ($C_{16}H_{10}^+$). Figure 3(b) and figure 3(c) are the projections of the PSD images selected for neutrals emitted only during the first revolution period after laser excitation at $t_{laser}$ = 0.5ms for anthracene ($C_{14}H_{10}^+$) and pyrene cations, respectively. The detection efficiency of a neutral fragment by the PSD strongly depends on its kinetic energy. Assuming the velocity of the neutral fragment equals to that of the parent ion, the kinetic energy of $C_2H_2$ (m=26 a.m.u.) is 26 time higher than for H (m=1 a.m.u.). For anthracene cation (m=178 a.m.u.) stored at 12keV kinetic energy, the detection efficiency of the lighter fragment H at lower kinetic energy (<100eV) is estimated to be less than 5% [19] while it is estimated to about 40% for $C_2H_2$ [20]. Moreover, the collection efficiency for the H loss channel is also reduced due to the kinetic energy release (KER). The average KER for this channel was measured from mass-analyzed ion kinetic-energy spectra (MIKES) to be 0.35eV for pyrene [21]. Based on this value, the diameter of the spot of the neutrals H hitting the PSD was calculated to be about 4cm, a value larger than the diameter (2.5 cm) of the detector. For anthracene cation, comparable dissociation rates are observed for both H and $C_2H_2$ channels [18]. Due to the very low detection and reduced collection efficiencies for H fragment, impacts recorded with the PSD were mainly attributed to the emitted $C_2H_2$ neutrals. Based on this assumption, a maximum KER of 0.5±0.2 eV was measured from the spot diameter on the PSD [22]. This value is in good agreement with previous MIKES measurement [18] and support the attribution of the detected fragments to $C_2H_2$ emission for anthracene cation (figure 3(b)). For pyrene cation the PSD image and its projection clearly exhibits two components. The main intense spot is attributed to $C_2H_2$ emission, similar as the anthracene case. The second component, superimposed to the main spot is attributed to H emission. Indeed branching ratios of 1.3%/98.5% was measured for the $C_2H_2$/H channels [23]. Despite the low detection and collection efficiencies of the emitted H fragment, this channel could be detected in the case of pyrene due to its high branching ratio. For two other PAH molecules, we have noticed that the PSD image

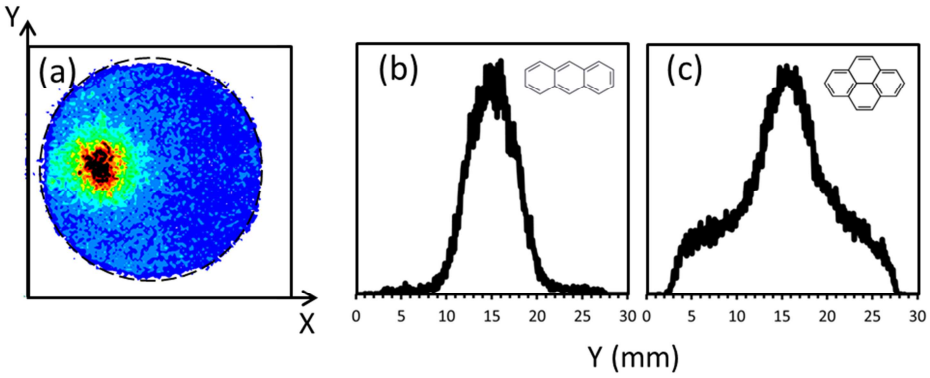


**Figure 3**. (a) PSD image for neutrals emitted by stored pyrene cations ($C_{16}H_{10}^+$) (b) projection of the PSD image for stored anthracene cations ($C_{14}H_{10}^+$) (c) projection of the PSD image for stored pyrene cations ($C_{16}H_{10}^+$).

obtained for naphthalene ($C_{10}H_8^+$) presents the same characteristic as for anthracene while for coronene ($C_{24}H_{12}^+$) the intensity of the signal attributed to $C_2H_2$ is drastically reduced. For the cata-condensed PAH, naphthalene and anthracene, the emission of $C_2H_2$ is indeed considered as an important channel while for the more compact structure of the peri-condensed pyrene and coronene molecules the loss of H is the dominant channel.

Successive loss of H from pyrene cation $C_{16}H_{10}^+$ has been investigated by storing successively $C_{16}H_{10-n}^+$ (n=0 - 4) within the Mini-Ring. The mass spectrum of ions extracted from the ECR source is presented in Figure 4(a). Figures 4(b)-(f) present the partial projections of the PSD images obtained by recording the emitted neutrals during 70μs after laser excitation of the stored ions at $t_{laser}$ = 0.5ms. The projections have been normalized to the intensity of the main peak attributed to the detection of $C_2H_2$ fragments. The ratio between the intensity of the main peak and the intensity of the component attributed to the loss of H provides qualitative information on the $C_2H_2$/H branching ratios of the $C_{16}H_{10-n}^+$ parent ion. The intensity of the signal attributed to the H loss channel decreases with the dehydrogenation of the parent molecular ion except for $C_{16}H_7^+$. For $C_{16}H_7^+$ this intensity is close to the one observed for $C_{16}H_9^+$. This is interpreted as a higher dissociation probability via H loss for $C_{16}H_9^+$ and $C_{16}H_7^+$. This interpretation is corroborated by recent calculations on the dissociation energies for the successive loss of H from pyrene cation [23]. The dissociation energies exhibit an odd-even effect with lower dissociation energy for $C_{16}H_9^+$ and $C_{16}H_7^+$ (table 1) indicating a lower stability of these molecular ions. This feature is expected as the lowest energy structures with an even number of empty hydrogen sites always have them paired [23]. This is also observed in the alternation of the peak intensity of the mass spectrum (figure 4(a)). The decay curve of the neutral signal associated to H emission can be obtained using a gate on the PSD (not shown). It is noteworthy that the same odd-even effect is observed with a faster decay of the neutral yield for $C_{16}H_9^+$ and $C_{16}H_7^+$. This observation supports our interpretation.

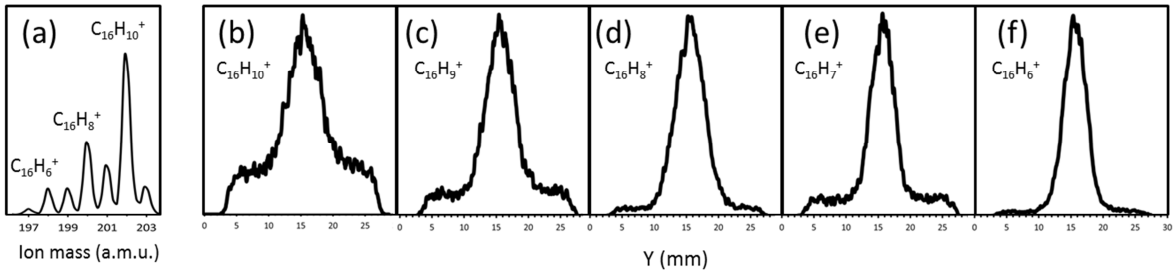


**Figure 4.**(a) mass spectrum for pyrene ions, (b)-(f) partial projections of the PSD image for neutrals emitted by stored $C_{16}H_{10-n}^+$ (n=0 - 4). The projections have been normalized to the intensity (arbitrary units) of the main peak.

**Table 1.** Calculated dissociation energies (eV) for H and $C_2H_2$ loss from $C_{16}H_{10-n}^+$ (n=0-4) parent ions (from [23]).

| Parent ion | H loss | $C_2H_2$ loss |
|---|---|---|
| $C_{16}H_{10}^+$ | 5.10 | 6.02 |
| $C_{16}H_9^+$ | 3.50 | |
| $C_{16}H_8^+$ | 4.48 | 6.00 |
| $C_{16}H_7^+$ | 4.11 | |
| $C_{16}H_6^+$ | 4.45 | |

## 4. Conclusion

PAH radiative cooling and fragmentation kinematics were studied using an electrostatic storage ring, the Mini-Ring. The time evolution of the internal energy distribution of the stored ions was probed using laser induced photo-dissociation. The observed fast radiative cooling is attributed to fluorescence from thermally excited electronic state populated via inverse internal conversion. By detecting the emitted neutral fragments with a position sensitive detector, information on the fragmentation channels and their qualitative branching ratios were obtained. Coincidence measurements between the neutral fragment and the charged daughter ion are planned in the future to unambiguously assign the observed decay channels.

## Acknowledgments

This work has been supported by the ANR 2010-042601“ANNEAU”.

## References

[1] Tielens A G G M 2013 *Rev. Mod. Phys.* **85** 1021
[2] Draine B T and Li A 2001 *Astrophys. J.* **551** 807
[3] Cami J, Bernard-Salas J, Peeters E and Malek S E 2010 *Science* **329** 1180
[4] Kwok S and Zhang Y 2011 *Nature* **479** 80
[5] Li A and Draine B T 2012 *Astrophys. J. Lett.* **760** L35
[6] Allain T, Leach S and Sedlmayr E 1996 *Astron. Astrophys.* **305** 602
[7] Léger A, Boissel P and d’Hendecourt L 1988 *Phys. Rev. Lett.* **60** 921
[8] Jochims H W, Ruhl E, Baumgartel H, Tobita S and Leach S 1994 *Astrophys. J.* **420** 307
[9] Dyakov Y A, Ni C, Lin S H, Lee Y T and Mebel A M 2006 *Phys. Chem. Chem. Phys.* **8** 1404
[10] Holm A I S, Johansson H A B, Cederquist H and Zettergren H 2011 *J. Chem. Phys.* **134** 044301
[11] Boissel P, de Parseval P, Marty P and Lefèvre G 1997 *J. Chem. Phys.* **106** 4973
[12] Andersen J U, Gottrup C, Hansen K, Hvelplund P and Larsson M O 2001 *Eur. Phys. J. D* **17** 189
[13] Ito G, Furukawa T, Tanuma H, Matsumoto J, Shiromaru H, Majima T, Goto M, Azuma T and Hansen K 2014 *Phys. Rev. Lett.* **112** 183001
[14] Martin S, Bernard J, Brédy R, Concina B, Joblin C, Ji M, Ortega C and Chen L 2013 *Phys. Rev. Lett.* **110** 063003
[15] Chen L, Ji M, Bernard J, Brédy R, Concina B, Joblin C, Ortega C, Montagne G and Martin S 2014 *J. Phys.: Conf. Series* **488** 012039
[16] Bernard J, Montagne G, Brédy R, Terpend-Ordacière B, Bourgey A, Kerleroux M, Chen L, Schmidt H T, Cederquist H and Martin S 2008 *Rev. Sci. Instrum.* **79** 075109
[17] Ji M, Brédy R, Chen L, Bernard J, Concina B, Montagne G, Cassimi A and Martin S 2013 *Phys. Scr.* **T156** 014091
[18] Ling Y and Lifshitz C 1998 *J. Phys. Chem. A* **102** 708
[19] Peko B and Stephen T 2000 *Nucl. Instrum. Methods Phys. Res., Sect B* **171** 597
[20] Takahashi N, Adachi Y, Saito M and Haruyama Y 2013 *Nucl. Instrum. Methods Phys. Res., Sect B* **315** 51
[21] Ling Y Y, Gotkis Y and Lifshitz C 1995 *Eur. J. Mass Spectrom.* **1** 41
[22] Ji M, Montagne G, Brédy R, Bernard J, Chen L and Martin S 2013 *Phys. Scr.* **T156** 014092
[23] West B, Useli-Bacchitta F, Sabbah H, Blanchet V, Bodi A, Mayer P M and Joblin C 2014 *J. Phys. Chem. A* **118** 7824